JOURNAL OF COMPUTATIONAL PHYSICS **128,** 254–258 (1996)
ARTICLE NO. 0207

NOTE

Comments on a Collocation Spectral Solver for the Helmholtz Equation

We present a simple extension of the spectral-collocation Helmholtz solver that was first derived by Ehrenstein and Peyret [3]. Ehrenstein and Peyret considered the case of a Helmholtz equation with constant coefficients under Dirichlet boundary conditions. We derive the more general case of nonhomogeneous, Robin boundary conditions. For simplicity, our discussion is restricted to the one-dimensional case

$$\frac{d^2u}{dx^2} - au = f, \quad x \in [-1, +1], \tag{1}$$

where a is a constant which is assumed to be ≥ 0. To solve this equation we impose the boundary conditions

$$\alpha_{\pm}u + \beta_{\pm}\frac{du}{dx} = g_{\pm}, \quad \text{at } x = \pm 1, \tag{2}$$

and discretize the interval $[-1, 1]$ by using the Gauss–Lobatto grid (see Canuto [2])

$$x_i = \cos\left(\frac{i\pi}{N}\right), \quad i \in \{0, ..., N\}. \tag{3}$$

Denoting $u(x_i)$ by u_i, one can compute the derivative of u_i with the equation

$$\frac{du_i}{dx} = \sum_{l=0}^{N} = d_{il}^{(1)}u_l, \tag{4}$$

where the analytic forms of $d_{ij}^{(1)}$, are derived in Gottlieb *et al.* [5]. Similarly,

$$\frac{d^2u_i}{dx^2} = \sum_{l=0}^{N} d_{il}^{(2)}u_l, \tag{5}$$

where it is possible to compute the $d_{ij}^{(2)}$ components by simply applying Eq. (4) twice. Alternatively, one can use the analytic formulae found in Zhao andYedlin [11]. To improve accuracy, one can also use the modifications outlined in Bayliss *et al.* [1].

We now have enough mathematical machinery to solve for u_i. We begin by solving for u_0 and u_N. Substituting Eq. (4) into Eq. (2) gives us

$$u_0 = \frac{Q}{\Delta} + \frac{\sum_{l=1}^{N-1}\kappa_{0l}u_l}{\Delta}, \tag{6}$$

and

$$u_N = \frac{R}{\Delta} + \frac{\sum_{l=1}^{N-1}\kappa_{Nl}u_l}{\Delta}, \tag{7}$$

where

$$Q = (\alpha_- + \beta_- d_{NN}^{(1)})g_+ - \beta_+ d_{0N}^{(1)}g_-, \tag{8}$$

$$R = (\alpha_+ + \beta_+ d_{00}^{(1)})g_- - \beta_- d_{N0}^{(1)}g_+, \tag{9}$$

$$\Delta = (\alpha_+ + \beta_+ d_{00}^{(1)})(\alpha_- + \beta_- d_{NN}^{(1)}) - \beta_+\beta_- d_{0N}^{(1)}d_{N0}^{(1)}, \tag{10}$$

$$\kappa_{0l} = \beta_+\beta_- d_{0N}^{(1)}d_{Nl}^{(1)} - (\alpha_- + \beta_- d_{NN}^{(1)})\beta_+ d_{0l}^{(1)}, \tag{11}$$

and

$$\kappa_{Nl} = \beta_+\beta_- d_{N0}^{(1)}d_{0l}^{(1)} - (\alpha_+ + \beta_+ d_{00}^{(1)})\beta_- d_{Nl}^{(1)}. \tag{12}$$

As is clear from the structure of Eqs. (6) and (7), reasonable values for u_0 and u_N exist $\Leftrightarrow \Delta \neq 0$. As we show later, $\Delta \neq 0$ for most cases of interest.

To determine the remaining u_i, we return to the Helmholtz equation, Eq. (1), but now replace the second-order differential by its matrix-collocation equivalent

$$\sum_{l=0}^{N} d_{il}^{(2)}u_l - au_i = f_i, \quad i \in \{0, ..., N\}. \tag{13}$$

Substituting Eqs. (6) and (7) into the above equation gives

$$\sum_{l=1}^{N-1} C_{il}u_l - au_i = Z_i, \quad i \in \{1, ..., N-1\}, \tag{14}$$

0021-9991/96 $18.00

where

$$C_{il} = \frac{d_{i0}^{(2)}\kappa_{0l}}{\Delta} + d_{il}^{(2)} + \frac{d_{iN}^{(2)}\kappa_{Nl}}{\Delta}, \tag{15}$$

and

$$Z_i = f_i - \frac{d_{i0}^{(2)}Q}{\Delta} - \frac{d_{iN}^{(2)}R}{\Delta}. \tag{16}$$

We can factor the matrix $[C_{ij}]$ in the fashion

$$C_{il} = \sum_{j=1}^{N-1} \alpha_{ij}\lambda_j\alpha_{jl}^{-1}, \quad 1 \le i, l \le N-1, \tag{17}$$

where $[\alpha_{ij}]$ is an $(N-1)(N-1)$ matrix, whose ith column is the eigenvector corresponding to the ith eigenvalue λ_i of the matrix $[C_{ij}]$, and $[\alpha_{ij}^{-1}]$ is the inverse of $[\alpha_{ij}]$, i.e.,

$$\sum_{j=1}^{N-1} \alpha_{ij}\alpha_{jl}^{-1} = \sum_{j=1}^{N-1} \alpha_{ij}^{-1}\alpha_{jl} = \delta_{il}, \tag{18}$$

where δ_{il} is the Kronecker delta function.

The eigenvalues of $[C_{ij}]$ are real, distinct, and less than zero, provided that $\beta_+\beta_- \le 0$ (Gottlieb and Lustman [6]).

Substituting Eq. (17) into Eq. (14) gives

$$\sum_{l=1}^{N-1}\sum_{j=1}^{N-1} \alpha_{ij}\lambda_j\alpha_{jl}^{-1}u_l - au_i = Z_i. \tag{19}$$

Multiplying the above equation by α_{mi}^{-1} and summing over i enables us to rewrite Eq. (19) as

$$\sum_{j=1}^{N-1} \delta_{mj}\lambda_j w_j - aw_m = t_m, \quad m \in \{1, ..., N-1\}, \tag{20}$$

where

$$w_m = \sum_{l=1}^{N-1} \alpha_{ml}^{-1}u_l, \tag{21}$$

and

$$t_m = \sum_{i=1}^{N-1} \alpha_{mi}^{-1}Z_i, \tag{22}$$

We can easily solve Eq. (20) to find that

$$w_m = t_m/(\lambda_m - a), \tag{23}$$

and so

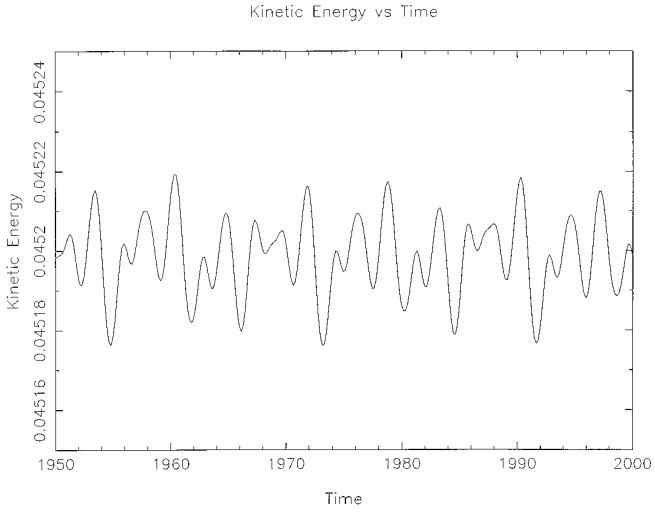

FIG. 1. The kinetic energy of the 2D Re = 10,000 driven cavity as a function of time.

$$u_j = \sum_{m=1}^{N-1} \alpha_{jm}w_m, \tag{24}$$

where the u_j are the solutions at the points x_j of Eqs. (1) and (2).

The generalization to the 2D case can be deduced from the discussion found in Zhao and Yedlin [11]. A numerical example of this method is given in the next section.

DRIVEN CAVITY

We wish to solve the normalized, two-dimensional, Navier–Stokes equation which has the form

$$\frac{\partial \mathbf{v}}{\partial t} = -\nabla p + \mathbf{N}(\mathbf{v}) + \frac{\nabla^2\mathbf{v}}{\mathrm{Re}}, \quad \text{in } \Omega, \tag{25}$$

subject to the incompressibility constraint

$$\nabla \cdot \mathbf{v} = 0, \quad \text{in } \Omega, \tag{26}$$

where $\mathbf{v}$ is the velocity, p is the pressure, Re is the Reynolds number, Ω is the integration domain of interest, and $\mathbf{N}$ is the nonlinear operator, which is assumed to have the form

$$\mathbf{N}(\mathbf{v}) = -\tfrac{1}{2}[\mathbf{v}\cdot\nabla\mathbf{v} + \nabla(\mathbf{v}\mathbf{v})]. \tag{27}$$

This skew symmetric form is adopted to minimize aliasing errors (Zang [10]).

To solve the Navier–Stokes equation, we used a first-order version of the splitting method given in Karniadakis *et al.* [8]. The resulting algorithm required the solution of one Poisson equation with Neumann boundary conditions

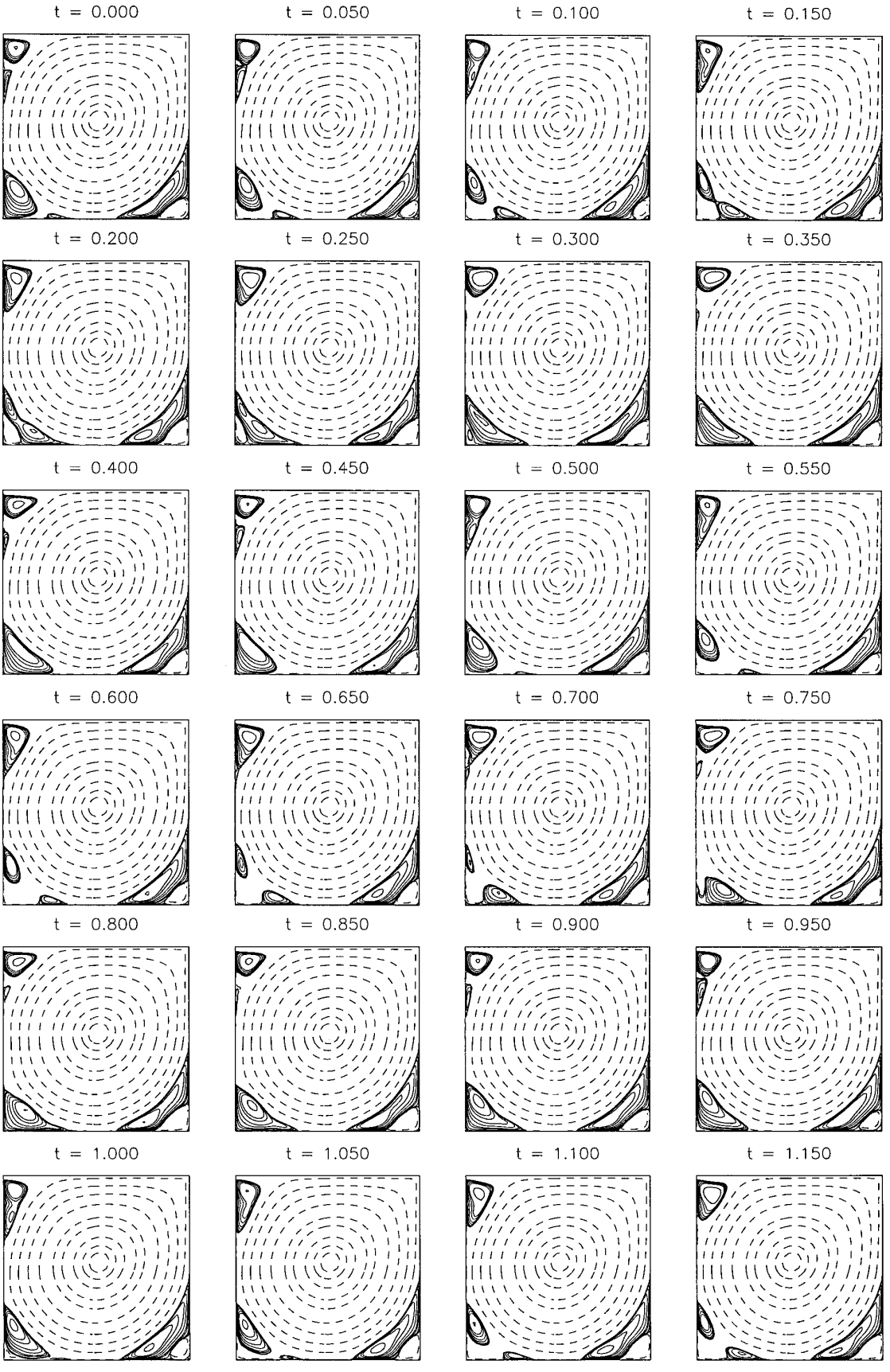

FIG. 2. Streamline depiction of approximately $\frac{1}{15}$ of one complete cycle for the 2D Re = 10,000 driven cavity.

and a vector Helmholtz equation with Dirichlet boundary conditions. The code was applied to a 2D driven cavity and the computed flow solutions for Re $\leq$ 5,000 compared well with those of Ghia *et al.* [4]. Ghia *et al.* computed steady-state solutions for driven cavity flows up to Re = 10,000. However, as discussed in Poliashenko and Aidun [9], the driven cavity goes unstable for Re $>$ 7,763. To illustrate these unstable flows, we computed the flow solution for Re = 10,000 driven cavity.

We set the initial velocity of the flow equal to zero throughout the domain of integration, except for the top "driving" lid, where we used a (u, v) velocity of

$$\mathbf{v} = (1 - \exp(-K(1 - x_i^2)), 0), \tag{28}$$

with $K = 20$. This particular form of driving lid has the advantage of removing the corner singularities from the traditional driven cavity. If we did not remove the corner singularities, the spectral code would suffer Gibbs oscillations (Gottlieb and Orszag [7]) and thereby undergo a major degradation in accuracy.

It took the code approximately 100 cpu hours on a SGI Personal Iris before the final asymptotic flow state was obtained. To determine when this occurred, we monitored the kinetic energy of the flow ($E(t)$), where the kinetic energy was given by

$$E(n\Delta t) = \frac{1}{2} \sum_{i=1}^{N_x-1} \sum_{j=1}^{N_y-1} A_{ij}[(u_{ij}^{(n)})^2 + (v_{ij}^{(n)})^2], \tag{29}$$

with N_x and N_y being the number of collocation points in the x and y directions ($N_x = N_y = 64$), and A_{ij} being the area (mass) associated with the point (x_i, y_j).

A close examination of the kinetic energy revealed a variation in the kinetic energy as a function of time (see Fig. 1). This shows the quasiperiodic nature of this unsteady flow, where the period of oscillation was found to be $\approx$17.5 time units.

Finally, in Fig. 2, a partial depiction of the unsteady Re = 10,000 driven cavity can be seen, where we show approximately $\frac{1}{15}$ of the quasiperiodic cycle that the cavity flow undergoes.

CONCLUSIONS

We have constructed a spectral solver for the Helmholtz equation using the Chebyshev collocation method. The solver, when applied to Helmholtz equations with constant (positive) coefficients and general boundary conditions, solves these equations in a direct (i.e., noniterative) manner.

As an illustrative example, we applied our solver to an unsteady Navier–Stokes problem and obtained a solution for the Re = 10,000, 2D driven cavity.

APPENDIX: CONDITIONS SUCH THAT $\Delta \neq 0$

For the solutions of the boundary values of u to be well defined, we require that $\Delta \neq 0$ (see Eq. (10)). In this section, we show that $\Delta \neq 0$ for most cases of interest.

For Dirichlet boundary conditions, ($\alpha_+, \alpha_- \neq 0$; $\beta_+ = \beta_- = 0$), we have $\Delta = \alpha_+\alpha_- \neq 0$, so we can always determine u_0 and u_N for such boundary conditions.

Neumann boundary conditions ($\alpha_+ = \alpha_- = 0$; $\beta_+, \beta_- \neq 0$), give

$$\Delta = \beta_+\beta_-[d_{00}^{(1)} d_{NN}^{(1)} - d_{0N}^{(1)} d_{N0}^{(1)}].$$

By using the analytic form for $d_{ij}^{(1)}$ (see Gottlieb *et al.* [5]), it is possible to show that $\Delta = 0 \Leftrightarrow N = 1$. In most spectral simulations N = 8, 16, 32, 64, ..., so we can be assured that $\Delta \neq 0$ in such circumstances.

Robin boundary conditions give 4 subcases to consider:

(a) $\alpha_+ = \beta_- = 0; \quad \alpha_-, \beta_+ \neq 0 \Rightarrow \Delta = \alpha_-\beta_+ d_{00}^{(1)} \neq 0$

(b) $\alpha_- = \beta_+ = 0; \quad \alpha_+, \beta_- \neq 0 \Rightarrow \Delta = \alpha_+\beta_- d_{NN}^{(1)} \neq 0$

(c) $\beta_+ = 0$; $\alpha_-, \alpha_+, \beta_- \neq 0$ gives

$$\Delta = 0 \Leftrightarrow N_c \equiv \frac{1}{\sqrt{2}} \left[\frac{6\alpha_-}{\beta_-} - 1 \right]^{1/2}, \tag{30}$$

where N_c is the value of N such that $\Delta = 0$. For the case $\beta_- = 0$, $\beta_+ \neq 0$, one obtains

$$\Delta = 0 \Leftrightarrow N_c \equiv \frac{1}{\sqrt{2}} \left[-\frac{6\alpha_+}{\beta_+} - 1 \right]^{1/2}, \tag{31}$$

(d) and finally, for $\alpha_+, \alpha_-, \beta_+, \beta_- \neq 0$

$$\Delta = 0 \Leftrightarrow N_c \equiv \frac{1}{\sqrt{2}} \left[\frac{3(\alpha_-\beta_+ - \alpha_+\beta_-)}{\beta_+\beta_-} \pm \frac{3\sqrt{(\alpha_-\beta_+ - \alpha_+\beta_-)^2 + 4\beta_+\beta_-(\alpha_+\alpha_- + \beta_+\beta_-/4)}}{\beta_+\beta_-} - 1 \right]^{1/2}. \tag{32}$$

The case for $\alpha_+ = 0$ (or $\alpha_- = 0$) and the rest non-zero, is included in Eq. (32). Clearly, for these more general boundary conditions, one has to ensure that $N \neq N_c$ so that $\Delta \neq 0$.

REFERENCES

1. A. Bayliss, A. Class, and B. J. Matkowsky, *J. Comput. Phys.* **116,** 380 (1994).
2. C. Canuto, M. Y. Hussaini, A. Quarteroni, and T. A. Zang, *Spectral Methods in Fluid Dynamics* (Springer-Verlag, New York, 1988).
3. U. Ehrenstein and R. Peyret, *Int. J. Numer. Methods Fluids* **9,** 427 (1989).
4. U. Ghia, K. N. Ghia, and C. T. Shin, *J. Comput. Phys.* **48,** 387 (1982).
5. D. Gottlieb, M. Y. Hussaini, and S. A. Orszag, ''Theory and Applications of Spectral Methods,'' in *Spectral Methods for Partial Differential Equations,* edited by R. G. Voigt, D. Gottlieb, and M. Y. Hussaini (SIAMCBMS, Philadelphia, 1984).
6. D. Gottlieb and L. Lustman, *SIAM J. Numer. Anal.* **20,** 909 (1983).
7. D. Gottlieb and S. A. Orszag, *Numerical Analysis of Spectral Methods: Theory and Applications* (SIAM monograph No. 26, Philadelphia, 1977).
8. G. E. Karniadakis, M. Israeli, and S. A. Orszag, *J. Comput. Phys.* **97,** 414 (1991).
9. M. Poliashenko and C. K. Aidun, *J. Comput. Phys.* **121,** 24 (1995).
10. T. A. Zang, *App. Num. Math.* **7,** 27 (1991).
11. S. Zhao and M. J. Yedlin, *J. Comput. Phys.* **113,** 215 (1994).

KURT LIFFMAN

Advanced Fluid Dynamics Laboratory
CSIRO/DBCE
P.O. Box 56
Highett, Victoria 3190
Australia